ORGANIC LETTERS

2012
Vol. 14, No. 23
5908–5911

Bis-Silylation of $Lu_3N@I_h$-C_{80}: Considerable Variation in the Electronic Structures

Kumiko Sato,[†] Masahiro Kako,*[,‡] Naomi Mizorogi,[†] Takahiro Tsuchiya,[†] Takeshi Akasaka,*[,†] and Shigeru Nagase*[,§]

Life Science Center of Tsukuba Advanced Research Alliance, University of Tsukuba, Ibaraki 305-8577, Japan, Department of Engineering Science, The University of Electro-Communications, Chofu 182-8585, Japan, and Fukui Institute for Fundamental Chemistry, Kyoto University, Kyoto 606-8103, Japan

kako@e-one.uec.ac.jp; akasaka@tara.tsukuba.ac.jp; nagase@ims.ac.jp

Received October 15, 2012

ABSTRACT

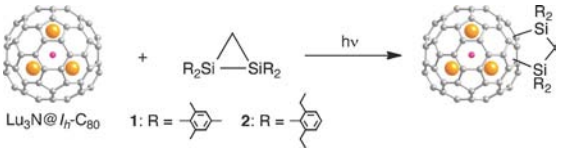

Photochemical reactions of $Lu_3N@I_h$-C_{80} with disiliranes 1 and 2 produce several isomeric adducts. Spectroscopic analyses characterize the most stable isomers as 1,4(AA) adducts, which consist of paired twist conformers at rt. The electrochemical and theoretical studies reveal that the HOMO−LUMO energy gaps of the 1,4(AA) adducts are smaller than that of $Lu_3N@I_h$-C_{80} because the electron-donating groups effectively raise the HOMO levels.

Endohedral metallofullerenes (EMFs) are of great interest because of their unique electronic structures, in which the encaged species and the carbon cages are regarded as having cationic and anionic characters, respectively. To date, exohedral chemical functionalization of EMFs and hollow fullerenes have been developed as powerful tools to modify the physical and chemical properties of EMFs[1] for various applications such as molecular electronics, nanomaterials sciences,[2] and biomedicine.[3] In this context, introduction of heteroatoms such as electropositive silicon onto fullerene surfaces has been recognized to affect the electronic characteristics of fullerenes.[4] Functionaization of EMFs and hollow fullerenes with disiliranes,[5] siliranes,[6] and silylenes[7] affords the corresponding silylated derivatives, which are proven to have negatively charged cage characters by electrochemical analyses and theoretical calculations. It is notable that the dynamic behavior of the

[†] University of Tsukuba.
[‡] The University of Electro-Communications.
[§] Kyoto University.

(1) (a) *Endofullerenes: A New Family of Carbon Clusters*; Akasaka, T., Nagase, S., Eds.; Kluwer: Dordrecht, The Netherlands, 2002. (b) Martín, N. *Chem. Commun.* **2006**, 2093–2104. (c) Dunsch, L.; Yang, S. *Phys. Chem. Chem. Phys.* **2007**, *9*, 3067–3081. (d) Dunsch, L.; Yang, S. *Small* **2007**, *3*, 1298–1320. (e) Chaur, M. N.; Melin, F.; Ortiz, A. L.; Echegoyen, L. *Angew. Chem., Int. Ed.* **2009**, *48*, 7514–7538. (f) Tan, Y. Z.; Xie, S. Y.; Huang, R. B.; Zheng, L. S. *Nat. Chem.* **2009**, *1*, 450–460. (g) Yamada, M.; Akasaka, T.; Nagase, S. *Acc. Chem. Res.* **2010**, *43*, 92–102. (h) *Chemistry of Nanocarbons*; Akasaka, T., Wudl, F., Nagase, S., Eds.; Wiley: Chichester, U.K., 2010.

(2) (a) Kobayashi, S.; Mori, S.; Iida, S.; Ando, H.; Takenobu, T.; Taguchi, Y.; Fujiwara, A.; Taninaka, A.; Shinohara, H.; Iwasa, Y. *J. Am. Chem. Soc.* **2003**, *125*, 8116–8117. (b) Yasutake, Y.; Shi, Z.; Okazaki, T.; Shinohara, H.; Majima, Y. *Nano Lett.* **2005**, *5*, 1057–1060. (c) Tsuchiya, T.; Kumashiro, R.; Tanigaki, K.; Matsunaga, Y.; Ishitsuka, M. O.; Wakahara, T.; Maeda, Y.; Takano, Y.; Aoyagi, M.; Akasaka, T.; Liu, M. T. H.; Kato, T.; Suenaga, K.; Jeong, J. S.; Iijima, S.; Kimura, F.; Kimura, T.; Nagase, S. *J. Am. Chem. Soc.* **2008**, *130*, 450–451. (d) Ross, R. B.; Cardona, C. M.; Guldi, D. M.; Sankaranarayanan, S. G.; Reese, M. O.; Kopidakis, N.; Peet, J.; Walker, B.; Bazan, G. C.; Van Keuren, E.; Holloway, B. C.; Drees, M. *Nat. Mater.* **2009**, *8*, 208–212. (e) Sato, S.; Seki, S.; Luo, G.; Suzuki, M.; Lu, J.; Nagase, S.; Akasaka, T. *J. Am. Chem. Soc.* **2012**, *134*, 11681–11686.

(3) (a) Cagle, D. W.; Kennel, S. J.; Mirzadeh, S.; Alford, J. M.; Wilson, L. J. *Proc. Natl. Acad. Sci. U.S.A.* **1999**, *96*, 5182–5187. (b) Fatouros, P. P.; Corwin, F. D.; Chen, Z.-J.; Broaddus, W. C.; Tatum, J. L.; Kettenmann, B.; Ge, Z.; Gibson, H. W.; Russ, J. L.; Leonard, A. P.; Duchamp, J. C.; Dorn, H. C. *Radiology* **2006**, *240*, 756–764.

(4) (a) Wakahara, T.; Kako, M.; Maeda, Y.; Akasaka, T.; Kobayashi, K.; Nagase, S. *Curr. Org. Chem.* **2003**, *7*, 927–943. (b) Nagatsuka, J.; Sugitani, S.; Kako, M.; Nakahodo, T.; Mizorogi, N.; Ishitsuka, M. O.; Maeda, Y.; Tsuchiya, T.; Akasaka, T.; Gao, X.; Nagase, S. *J. Am. Chem. Soc.* **2010**, *132*, 12106–12120 and references cited therein.

10.1021/ol302832k
Published on Web 11/12/2012

encapsulated metal atoms in the EMF cages can be regulated by exohedral functionalization. In fact, the motion of La atoms inside the bis-silylated $La_2@I_h$-C_{80} is restricted to two dimensions because of perturbation of the electrostatic potentials inside the cage caused by the electropositive silyl groups.[5c]

Recently, $Lu_3N@I_h$-C_{80} has been reported to react with thermally generated bis(2,6-diethylphenyl)silylene, a divalent silicon species, to afford a [6,6]-silacyclopropane adduct, which isomerizes subsequently into a [5,6]-silafulleroid derivative.[7] The electrochemistry of silylene derivatives shows the weak effects of monosilylation on the redox potentials, compared to the case of bis-silylated $Sc_3N@I_h$-C_{80}.[5b] However, the reaction of silylene with $Sc_3N@I_h$-C_{80} did not proceed efficiently to afford the corresponding adducts in quite low yields. Consequently, it is important to investigate the effects of the various silyl groups onto $Lu_3N@I_h$-C_{80} cages. This report demonstrates the reactions of $Lu_3N@I_h$-C_{80} with disiliranes **1** and **2**, which produce several $Lu_3N@I_h$-$C_{80}(R_2Si)_2CH_2$ regioisomers (Scheme 1). The electrochemical study and theoretical calculation were also conducted to reveal the electronic properties of the silylated EMFs. Additionally, we describe the novel isomerization of the disilirane adducts observed in this study.

Scheme 1. Synthesis of $Lu_3N@I_h$-$C_{80}(R_2Si)_2CH_2$ Derivatives

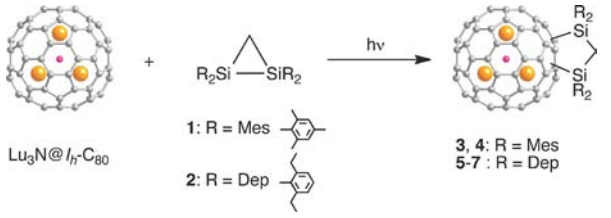

Photoreaction of $Lu_3N@I_h$-C_{80} and **1** was carried out in a mixed solvent of 1,2-dichlorobenzene/toluene using a 500 W halogen lamp. Subsequent preparative HPLC separation afforded products **3** and **4** in 59% and 21% yields, respectively (Figures S1 and S2 in the Supporting Information). MALDI-TOF mass spectrometry (Figure S6) of **3** and **4** displays molecular ion peaks at m/z 2045 (M^-), as expected for 1:1 adducts of $Lu_3N@I_h$-C_{80} and **1**. A base peak at m/z 1499 is also observed as the fragment ion $Lu_3N@I_h$-C_{80}^-. In a similar procedure, photoreaction of $Lu_3N@I_h$-C_{80} and **2** gave two products **5** and **6** in 49% and 12% yields, respectively (Figures S3 and S4). In addition, **4** and **6** were photolabile to isomerize into **3** and **5**, respectively, under ambient light (Figures S7 and S8). Furthermore, an intermediate **7** was observed in the transformation of **6** to **5** in the dark, even at 25 °C (Figure S9). The MALDI-TOF mass measurement of **5**–**7** also verified the formation of 1:1 adducts derived from **2**. NMR analyses of **3**, **5**, and **7** were conducted as follows whereas those of **4** and **6** were difficult because of the instability.

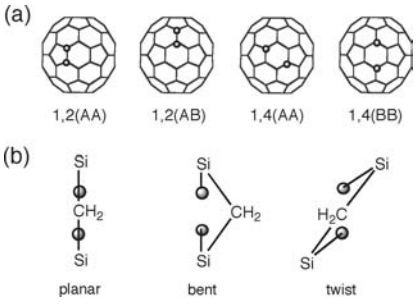

Figure 1. Addition patterns. (a) Four possible addition sites for 1,2-addition and 1,4-addition. (b) Three conformations of disilirane moiety.

Because two kinds of nonequivalent carbon atoms exist on the I_h-C_{80} cage, the possible addition sites for 1,2- and 1,4-addition are as follows: 1,2(AA), 1,2(AB), 1,4(AA), 1,4(BB) (Figure 1a). The $(Mes_2Si)_2CH_2$ addend in **3** can adopt three conformations, as depicted in Figure 1b. The possible isomers and symmetries expected for I_h-$C_{80}(Mes_2Si)_2CH_2$ are presented in Table S1 in the Supporting Information. The ^1H, ^{13}C, and 2D NMR spectra of **3** indicate that **3** involves two conformers (**3-I** and **3-II**) in the ratio 5:2 (Figures S10 and S11). Each conformer shows four aryl proton signals, six methyl signals, and one methylene signal. In addition, two sets of 39 sp^2 carbon signals and 1 sp^3 carbon signal of the I_h-C_{80} cage are observed for each of the conformers as shown in the ^{13}C NMR. Four tertiary and eight quarternary mesityl ring carbon signals, one methylene carbon signal, and six methyl carbon signals are also found for each of the conformers. For further structural determination of **3**, VT-^1H NMR analyses were performed between 243 and 343 K (Figure S12). As expected, the signals of the two conformers coalesced to afford a simple spectrum at 343 K. Subsequently, when the NMR sample was cooled to 243 K, the spectrum before heating was observed again. The NMR spectra of **3** including the VT experiments suggest that the symmetry of **3** is C_2 at 343 K. These spectral properties closely resemble those of [1,4]-$Sc_3N@I_h$-$C_{80}(Mes_2Si)_2CH_2$.[5b] Therefore, **3** seems to be the 1,4(AA) adduct, which has two twist conformers. The coalescence of NMR signals at 343 K is rationalized by the rapid interconversion between the conformers. 2D EXSY

(5) (a) Yamada, M.; Nakahodo, T.; Wakahara, T.; Tsuchiya, T.; Maeda, Y.; Akasaka, T.; Kako, M.; Yoza, K.; Horn, E.; Mizorogi, N.; Kobayashi, K.; Nagase, S. *J. Am. Chem. Soc.* **2005**, *127*, 14570–14571. (b) Wakahara, T.; Iiduka, Y.; Ikenaga, O.; Nakahodo, T.; Sakuraba, A.; Tsuchiya, T.; Maeda, Y.; Kako, M.; Akasaka, T.; Yoza, K.; Horn, E.; Mizorogi, N.; Nagase, S. *J. Am. Chem. Soc.* **2006**, *128*, 9919–9925. (c) Wakahara, T.; Yamada, M.; Takahashi, S.; Nakahodo, T.; Tsuchiya, T.; Maeda, Y.; Akasaka, T.; Kako, M.; Yoza, K.; Horn, E.; Mizorogi, N.; Nagase, S. *Chem. Commun.* **2007**, 2680–2682. (d) Yamada, M.; Wakahara, T.; Tsuchiya, T.; Maeda, Y.; Kako, M.; Akasaka, T.; Yoza, K.; Horn, E.; Mizorogi, N.; Nagase, S. *Chem. Commun.* **2008**, 558–560.

(6) Yamada, M.; Minowa, M.; Sato, S.; Kako, M.; Slanina, Z.; Mizorogi, N.; Tsuchiya, T.; Maeda, Y.; Nagase, S.; Akasaka, T. *J. Am. Chem. Soc.* **2010**, *132*, 17953–17960.

(7) Sato., K.; Kako, M.; Suzuki, M.; Mizorogi, N.; Tsuchiya, T.; Olmstead, M. M.; Balch, A. L.; Akasaka, T.; Nagase, S. *J. Am. Chem. Soc.* **2012**, *134*, 16033–16039.

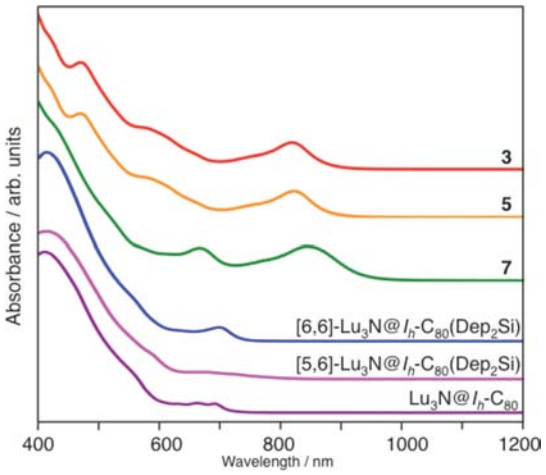

Figure 2. Vis−NIR absorption spectra of $Lu_3N@I_h$-C_{80}, disilirane, and silylene derivatives.

NMR measurement was performed using the phase sensitive NOESY pulse sequence to confirm the interrelation between these conformers (Figure S13). The spectrum showed several cross-peaks corresponding to the conformers indicating the chemical exchange between the conformers.

The ^{13}C NMR spectra of **5** show two sets of 39 sp^2 carbon signals and 1 sp^3 carbon signal of the I_h-C_{80} cage in the ratio 1:1, which closely resemble those of **3** (Figure S14). In addition, the HMBC spectrum shows that two singlet proton signals, assignable to Si−CH_2−Si at 2.09 and 2.29 ppm, correlate with two sp^3 cage carbons at 59.36 and 58.88 ppm. Moreover, HSQC measurement shows that these two singlet proton signals have two cross-peaks at 13.54 and 15.90 ppm (Figure S15). These observations indicate that **5** has C_2 symmetry with two conformers, **5-I** and **5-II** as in the case of **3**. Unfortunately, the coalescence of signals of **5** in the VT-^1H NMR was not observed up to 353 K, probably because of steric restrictions caused by the bulky Dep groups (Figure S16). Based on symmetry considerations, the structure of **5** was determined as a 1,4(AA) adduct, coupled together with the vis−NIR spectral observation as described below.

The ^{13}C NMR spectrum of **7** shows four quartet signals for CH_3 and four triplet signals for CH_2 of ethyl groups, and one triplet for the Si−CH_2−Si moiety, as well as 51 sp^2 carbons. A singlet signal for the sp^3 carbon of the I_h-C_{80} cage was also observed at 49.24 ppm (Figure S17). These spectral data suggest that **7** is a 1,4-adduct with C_2 symmetry, but it is not clear whether **7** is a 1,4(AA) or a 1,4(BB) adduct. A singlet signal for the sp^3 carbon of the I_h-C_{80} cage was observed at 49.24 ppm, with a chemical shift of ~10 ppm upfield compared to those of **5**. This observation

Table 1. Redox Potentials (V)[a] and HOMO/LUMO Levels (eV)[b] of **3**, **5**, and Related I_h-C_{80} EMFs

compd	$E^{ox}{}_1$	$E^{red}{}_1$	$E^{red}{}_2$	$E^{red}{}_3$	HOMO	LUMO
$Lu_3N@I_h$-C_{80}	+0.61	−1.39[c]	−1.83[c]	−2.16[c]	−6.49	−2.38
3	+0.06[c]	−1.55[c]	−2.01[c]			
3-I					−5.65	−2.10
3-II					−5.68	−2.05
5	+0.08[c]	−1.61[c]	−2.15[c]	−2.58[c]		
5-I					−5.70	−2.14
5-II					−5.71	−2.10
8[d,e]	+0.27[c]	−1.43[c]	−1.72[c]	−1.94[c]		
9[d,f]	+0.43[c]	−1.52[c]	−1.73[c]	−1.99[c]		
$Sc_3N@I_h$-C_{80}[g]	+0.62	−1.22			−6.47	−2.58
10[g,h]	+0.08[c]	−1.45				

[a] Values obtained by DPV are in volts relative to the ferrocene/ferrocenium couple. [b] See ref 11. [c] Irreversible. [d] Data from ref 7. [e] **8** = [5,6]-$Lu_3N@I_h$-$C_{80}(Dep_2Si)$. [f] **9** = [6,6]-$Lu_3N@I_h$-$C_{80}(Dep_2Si)$. [g] Data from ref 5b. [h] **10** = [1,4]-$Sc_3N@I_h$-$C_{80}(Mes_2Si)_2CH_2$.

suggests that the addition site of **7** is 1,4(BB) with C_2 symmetry.

The vis−NIR spectroscopy offers valuable information about structures of exohedrally functionalized EMFs.[8] The spectra of **3** and **5** show distinctive absorption maxima at 807 and 810 nm (Figure 2), respectively, which closely resemble that of the reported [1,4]-$Lu_3N@I_h$-$C_{80}(CH_2C_6H_5)_2$.[9] It is noteworthy that the spectra of **3** and **5** differ much from those of $Lu_3N@I_h$-$C_{80}(Dep_2Si)$, which have been determined to be 1,2-adducts at the [6,6]- and [5,6]-ring junctions, respectively.[7] Consequently, these spectroscopic data, including ^{13}C NMR and vis−NIR, support the structures of **3** and **5** as a 1,4(AA) twist adduct. However, the spectrum of **7** differs somewhat from those of **3** and **5**, showing absorption maxima at 666 and 840 nm. Therefore, we tentatively assigned a 1,4(BB) twist structure to **7** based on the NMR and vis−NIR spectra.

The electrochemical behaviors of **3** and **5** were studied using cyclic voltammetry (CV) and differential pulse voltammetry (DPV). The voltammograms of **3** and **5** show that both the oxidation and reduction process are irreversible (Figure S18).[10] As shown in Table 1, the first oxidation ($E^{ox}{}_1$) and the first reduction ($E^{red}{}_1$) potentials of **3** are shifted cathodically by 550 and 160 mV, respectively, compared with those of $Lu_3N@I_h$-C_{80}. For adduct **5**, the cathodic shifts of $E^{ox}{}_1$ and $E^{red}{}_1$ are, respectively, 530 and 220 mV. These cathodic shifts of the redox potentials are quite similar to those observed for the cases of [1,4]-$Sc_3N@I_h$-$C_{80}(Mes_2Si)_2CH_2$.[5b] Therefore, the [1,4]-bissilylated structures of **3** and **5** are also supported by the electrochemical properties. However, the redox potentials of [6,6]- and [5,6]-$Lu_3N@I_h$-$C_{80}(Dep_2Si)$[7] show less cathodic shifts compared to those of **3** and **5**, as expected from

(8) Exohedrally functionalized EMFs and hollow fullerenes show the corresponding characteristic vis−NIR spectra, which are specific to the regiochemistry of functionalization, and irrespective of the type of functional groups. For example, [1,4]-$Sc_3N@I_h$-$C_{80}(Mes_2Si)_2CH_2$[5b] and [1,4]-$Sc_3N@I_h$-$C_{80}(CH_2C_6H_5)_2$[9] afford very similar spectra with absorption maxima around 900 nm.

(9) Shu, C. Y.; Slebodnick, C.; Xu, L. S.; Champion, H.; Fuhrer, T.; Cai, T.; Reid, J. E.; Fu, W.; Harich, K.; Dorn, H. C.; Gibson, H. W. *J. Am. Chem. Soc.* **2008**, *130*, 17755–17760.

(10) Removal of the addend occurred during the electrochemical measurements of **3** and **5** to give pristine $Lu_3N@I_h$-C_{80}, as reported for [1,4]-$Sc_3N@I_h$-$C_{80}(Mes_2Si)_2CH_2$.[5b]

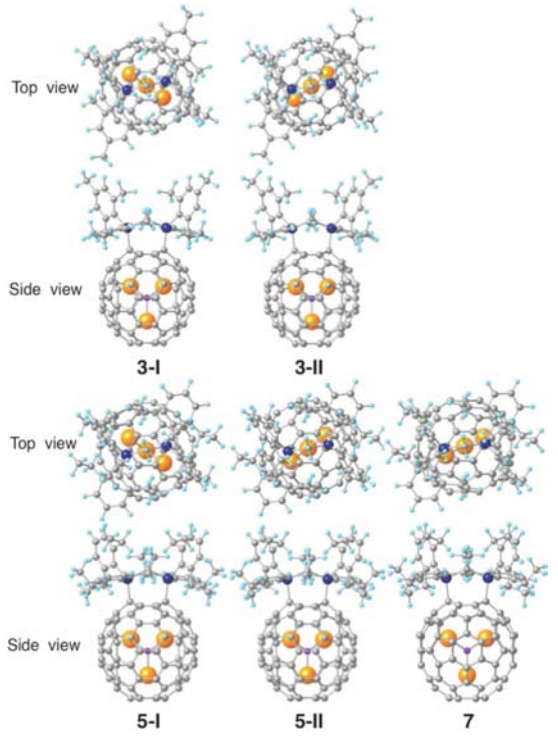

Figure 3. Optimized structures of $Lu_3N@I_h$-C_{80} disilirane derivatives.

the numbers of silicon atoms introduced onto the surface of the I_h-C_{80} cage.

To obtain more insight into the structures of **3**, **5** and **7**, the optimized structures of **3-I**, **II** and **5-I**, **II** are calculated based on those of [1,4]-$Sc_3N@I_h$-$C_{80}(Mes_2Si)_2CH_2$[5b] as shown in Figure 3.[11] Paired twist conformers are found to be almost isoenergetic: **3-I** is 1.1 kcal/mol less stable than **3-II**; in addition, **5-I** is 0.8 kcal/mol more stable than **5-II**. In contrast, the optimized structure of **7** was calculated as 10.4 kcal/mol less stable than **5-I** in agreement with the experimentally obtained result that **7** isomerizes readily to **5**.

(11) All calculations were performed with density functional theory at the M06-2X level[12] using the Gaussian09[13] program. SDD basis set[14] with the effective core potential was used for Lu, LanL2DZ basis set[15] for Sc, and 6-31G(d) basis set[16] for C, H, N, and Si.

(12) Zhao, Y.; Truhlar, D. G. *Theor. Chem. Acc.* **2008**, *120*, 215–241.

(13) Frisch, M. J.; et al. *Gaussian 09*, revision C.01; Gaussian, Inc.: Wallingford, CT, 2010.

Therefore, the structure of **7** is most likely to be a 1,4(BB) adduct, which was hitherto unknown for I_h-C_{80} based EMF derivatives. It is worthwhile to note that the optimized structures of **3** and **5**, by changing the orientation of the Lu_3N cluster, were less stable by 15−27 kcal/mol than either **3-I**, **II** or **5-I**, **II** (Figure S19). These results predict that free rotation of the Lu_3N cluster is restricted inside the cages.

The HOMO−LUMO energy levels of the calculated compounds also correlate well with the experimental cathodic shifts of the redox potentials (Table 1). Consequently, the calculation confirmed the remarkable difference in the electronic property between monosilylated and bis-silylated $Lu_3N@I_h$-C_{80} derivatives.

In conclusion, we report for the first time that several bis-silylated $Lu_3N@I_h$-C_{80} derivatives have been synthesized using photochemical additions of disiliranes. Interestingly, a facile transformation took place between the bis-silylated $Lu_3N@I_h$-C_{80}, in which the 1,4(AA) adducts are the most stable product. Electrochemical and theoretical studies of the 1,4(AA) adducts demonstrate that bis-silylation is more effective and versatile for tuning the π electronic characters of various EMFs than monosilylation using silylenes.

Acknowledgment. This work was supported by a Grant-in-Aid for Scientific Research on Innovative Areas (No. 20108001, "pi-Space"), a Grant-in-Aid for Scientific Research (A) (No. 20245006) and (B) (No. 24350019), The Next Generation Super Computing Project (Nanoscience Project), Nanotechnology Support Project, Grants-in-Aid for Scientific Research on Priority Area (Nos. 20036008 and 20038007), Specially Promoted Research (No. 22000009) from the Ministry of Education, Culture, Sports, Science, and Technology of Japan, and The Strategic Japanese−Spanish Cooperative Program funded by JST and MICINN.

Supporting Information Available. Experimental procedures, spectroscopic data, theoretical calculation data, and complete ref 13. This material is available free of charge via the Internet at http://pubs.acs.org.

(14) Cao, X. Y.; Dolg, M. *THEOCHEM* **2002**, *581*, 139–147.

(15) Hay, P. J.; Wadt, W. R. *J. Chem. Phys.* **1985**, *82*, 299–310.

(16) Hehre, W. J.; Ditchfield, R.; Pople, J. A. *J. Chem. Phys.* **1972**, *56*, 2257–2261.

The authors declare no competing financial interest.